American Journal of Pathology, Vol. 139, No. 2, August 1991

Cell Migration and Actin Organization in Cultured Human Primary, Recurrent Cutaneous and Metastatic Melanoma

Time-lapse and Image Analysis

H. Randolph Byers,* Takafumi Etoh,* Joanne R. Doherty,* Arthur J. Sober,† and Martin C. Mihm, Jr.*

From the Dermatopathology Division, Department of Pathology, and the Department of Dermatology,† Harvard Medical School, Massachusetts General Hospital, Boston, Massachusetts*

Random cell migration and actin organization in seven human primary, recurrent cutaneous, and metastatic melanoma cell lines were studied by time-lapse video recording and image analysis. The migration of over 800 randomly selected cells from the cell lines were recorded using an inverted microscope with an attached incubator housing. The fraction of cells with random migration rates greater than 10 μm/hour was 8% in an established primary melanoma cell line, 2% and 34% in two recurrent cutaneous melanoma cell lines, and 5%, 30%, 31%, and 60% in four metastatic cell lines. The three metastatic cell lines with significantly higher mean migration rates ($P < 0.001$) were derived from lymph node metastases, whereas the fourth metastatic cell line was derived from a visceral metastasis. The cellular morphology and presence of cell nests in the original tissue correlated with in vitro cell morphology and the formation of colonies. The ability of cells to organize actin into stress fibers directly correlated with significantly higher random migration rates and lack of colony formation. Characterization of random migration rates and actin organization of human melanoma cells that are isolated from different stages of tumor progression may lend insight into metastasis. (Am J Pathol 1991, 139:423–435)

Tumorigenesis and metastasis appear to involve a series of complex genotypic and phenotypic events. The association of human malignant melanoma *in situ* with dysplastic nevi and the appearance of the tumorigenic phase with the capacity for metastasis are pathologic or phenotypic steps in disease progression.[1–3] Invasive malignant melanoma is proposed to involve at least three steps: 1) capacity to bind the basement membrane; 2) ability to digest the basement membrane; and 3) capacity for cell migration.[4] The focus of the present study is on the latter step, and more specifically, to characterize the random melanoma cell migration and actin organization of a number of melanoma cell lines that we have isolated in recent years from different stages of progression.

Many investigators have identified model systems that indicate that cell motility may play a role in metastatic behavior. The *in vitro* organization of actin as well as locomotor activity has been reported to correlate with metastatic potential after tail vein injection into syngeneic or nude mice.[5–8] The finding of stable actin bundles also has been reported more frequently in low-metastatic variants of human melanoma, fibrosarcoma,[6,8] and adenocarcinoma cell lines.[9] In addition, cytoplasmic components associated with the disruption[9] or stabilization[10] of the actin architecture appears to alter the metastatic potential of adenocarcinoma cells.

A number of *in vitro* models have been recently developed to study cell motility of malignant cells. Melanoma cell migration through micropore filters coated with extracellular matrix proteins and use of Boyden chambers (differential media compartmentalization) has provided insight into cell–substrate adhesion as well as factors promoting motility.[4] Cell migration in a capillary tube assay system has allowed observation of the motility of single cells over greater distances than the micropore

Presented in part in abstract form only to meetings of the Society of Investigative Dermatology and the American Society of Cell Biology.

Supported by National Institutes of Health grant R29 CA45587 to H. R. Byers.

Accepted for publication April 12, 1991.

Address reprint requests to H. Randolph Byers, MD, PhD, Pathology Research, 7th Floor East, Massachusetts General Hospital, 149 13th St., Charlestown, MA 02129.

filter assay system, and correlation of carcinoma cell migratory rate with metastatic capability has been identified.[11,12] Visualization of spreading and migrating cells and their cytoskeletal proteins by immunofluorescent techniques, however, is optically hindered by these methods. In this study, we incorporate a computerized tissue culture assay system that follows the migration of many individual cells simultaneously over relatively large distances (tens of micrometers) and that is optically conducive to observe cell shape changes and cytoskeletal distribution.

We report the isolation of seven human melanoma cell lines from different stages of tumor progression and the use of a time-lapse video image analysis system for recording individual cell random migration and quantitation of cell shape and actin distribution. Our data show that these cell lines exhibit a remarkable heterogeneity of cell shape, actin organization, and cell migration rate and that high random migration rates directly correlate with capacity of the cell lines to form microfilament bundles in stress fiber arrays. The isolation of human melanoma cell lines from different stages of tumor progression with variable random migration rates and actin distribution may give insight into the control of migration by extracellular matrix proteins, expression of cell adhesion molecules, and cytoskeletal proteins.

Materials and Methods

Tissue Culture

Melanocytes

Human newborn foreskins were removed for routine circumcision and cultures were derived as previously described with slight modification.[13] Briefly, the tissue was rinsed in 70% ethanol and minced into 1-mm cubes and incubated in 0.25% trypsin and 0.02% ethylenediaminetetra-acetic acid (EDTA; Gibco, Grand Island, NY) in phosphate-buffered saline (PBS) for 1 hour while stirring at 37°C. The supernatant was decanted and centrifuged at 500*g* for 5 minutes and the cell pellet was resuspended in melanocyte growth media (Clonetics, San Diego, CA) containing bovine pituitary extract (0.2% vol/vol), phorbol 12-myristate 13-acetate (10 ng/ml), bovine insulin (5 μg/ml), hydrocortisone (0.5 μg/ml), and recombinant fibroblast growth factor (1 ng/ml). After 1 week, the cells were treated with Geneticin (G418 sulfate, Gibco) at a concentration of 100 μg/ml for 2 days to kill contaminating fibroblasts.[13]

Primary Melanoma (PM)

Cells were obtained from a sterile fresh surgical specimen of a primary cutaneous malignant melanoma, superficial spreading type. The radial growth phase (RGP) and vertical growth phase (VGP) of this primary melanoma (PM) from patient WK were dissected from approximately 10% of the original lesion and coded PMWK-R and PMWK-V, respectively. The tissue fragments were washed three times in calcium- and magnesium-free PBS and incubated in 0.25% trypsin at 37°C for 1 hour. The epidermis was then separated from the dermis using a dissecting microscope and the fragments minced into less than 1-mm cubes. The VGP culture was derived from explants of a small portion of the centrally located grossly identifiable nodule in the dermis, and the RGP cultures were obtained from explants of epidermis and fragments of papillary dermis 2 mm from the central nodule. The adjacent sites were examined histologically to confirm each growth phase.

Recurrent Primary Melanoma (RPM)

Two cell lines were established, one from patient EP (RPM-EP) and the other from patient MC (RPM-MC). The epidermis was removed as above and explant cultures were established.

Metastatic Melanoma (MM)

Four cell lines were obtained by explant culture. Cell lines MM-AN, MM-BP, and MM-RU were derived from inguinal, axillary, and cervical lymph nodes of patients AN, BP, and RU, respectively, whereas cell line MM-LH was derived from a visceral (omental) metastasis of patient LH.

Culture Media

All cells were cultured in minimal essential media with Earles balanced salt solution, with 0.5% Gentamicin (Gibco, cat # 600-5710 AD) and supplemented with 2% fetal calf serum and 8% newborn calf serum.

Characterization of Cell Lines

Cells grown on coverslips were fixed in 4% paraformaldehyde in PBS (pH 7.4), rinsed in PBS, and incubated for 10 minutes in PBS with 10% bovine serum albumin, then incubated in either polyclonal anti–S-100 protein antibody (Dako Corp., Santa Barbara, CA) or monoclonal anti–HMB-45 antibody (Enzo Diagnositics, Inc.) for 1 hour at 37°C. After three PBS washes, the secondary antibodies, peroxidase-conjugated anti-goat or anti-mouse antibodies were used, depending on the primary antibody, and the development of a reaction product with diaminobenzedine was performed using a kit (Dako Corp.).

Incubation with the peroxidase-labeled secondary antibody alone as well as staining of cultured normal human fibroblasts served as controls for the specificity of the immunolabeling characterization.

Proliferation rates or doubling times were calculated on the basis of cell number on equal seeding into multiwell plates, trypsinization every 2 to 3 days, and cell counts. Cells were counted in an automated cell counter (Coulter Electronics, Inc., Hialeah, FL). The formulas used for calculating the cell doubling time during the most rapid growth phase interval when slope (a) is maximal were as follows: where $\ln n_0$ is the natural logarithm of the number of cells at the initial time (t_0) and $\ln n_1$ is the natural logarithm of the number of cells at the end of the rapid growth phase (t_1):

$$\text{slope} = a = \frac{\Delta y}{\Delta x} = \frac{\ln n_1 - \ln n_0}{t_1 - t_0}$$

To calculating doubing time (Δt):

$$a = \frac{\ln 2n_0 - \ln n_0}{\Delta t}$$

$$a = \frac{\ln 2 + \ln n_0 - \ln n_0}{\Delta t}$$

$$\Delta t = \frac{\ln 2}{a}$$

Cell Migration, Cell Spreading Assay

Time-lapse Recording

Cell cultures were observed with a Nikon Diaphot inverted microscope with a 10× phase contrast objective, an attached hermetically sealed Plexiglas incubator housing, Nikon incubator (NP-2) with stage thermostat (Donsanto Corp., Natick, MA) and Sheldon Laboratory 2004 CO_2 flow mixer (Cornelius, OR) to obtain constant temperature (37°C) and pH (5% CO_2 and 95% air) indefinitely. A Dage-MTI model 65DX video camera (Michigan City, ID) with a Newvicon tube was attached to the camera port and connected to a Hitachi TLC1550 time-lapse video cassette recorder (Marcon Instruments, Norwood, MA).

Cell migration was recorded between 2 and 18 hours after plating onto sterile glass coverslips in 35-mm petri dishes (for immunofluorescence) or plastic culture dish surfaces (LUX, Nunc, Naperville, IL). Cell density was between 0.4 and 1.0 cells per 10,000 square micrometers to avoid possible effects of cell–cell interactions or other density-dependent phenomena. Using the 10× objective on the inverted microscope, between 13 and 57 individual cells were tracked on the video monitor with an analysis field of 650 × 960 μm. Cells that were rounded or divided during the recording interval were eliminated from the calculation of migration rate. Round cells were defined as exhibiting a concentric phase-contrast pattern with absence of phase-contrast processes or lamellipodia. These cells were found to be either: 1) not attached, 2) attached and dividing, or rarely, 3) attached, stationary, and nondividing for the duration of the recording period. Trypan blue exclusion testing of the round cells showed that the nonattached cells and a few of the stationary cells were nonviable. At no time did the number of these round cells or dividing cells exceed 10% of the total cells followed during the typical migration assay period of 4 hours. Each migration study was repeated between three and five times for each cell line.

Image Analysis

Over 820 cells were tracked for an average of more than 100 cells per cell line. Video images were played back at 60-minute intervals, for total time intervals from 4 to 8 hours. Video images of the intervals were digitally saved, and the individual direction and distance migration of each cell was analyzed using a Microcomp Image analysis system by Southern Micro Instruments (Atlanta, GA). The system used a Numonics digitablet and an IBM-compatible personal computer with an installed video card, 'PC Vision Plus Frame Grabber' from Imaging Technology (Woburn, MA) and a high-resolution video monitor (Sony, Inc., New York, NY).

For comparison of cell lines, migration rate was defined as the sum of hourly migration distances divided by the total elapsed time. A planar morphometry program was used for two-dimensional projected surface area of the cells to assess cell spreading (see Microcomp above). For distance and area measurements, the x- and y-axis computer pixel units of the system were calibrated with the inverted microscope objectives using a 0.01-mm slide micrometer. The data was saved as an MS DOS (Microsoft Corp, Redmond, WA) file and then translated through a TOPS network (A Sun Microsystems Co., Berkeley, CA) to Macintosh software and hardware for statistics and graphics. Statistical analysis of the migration rates was performed by using the Student's *t*-test on Statworks. Normalized migration paths (Figure 5) were obtained by 'grabbing' individual cell paths and 'dragging' the paths without rotation such that the origin of all paths are superimposed on one central point by using the program MacDraw.

Light Microscopy

Bright-field and Phase-contrast Microscopy

Paraffin-embedded, sectioned, and hematoxylin and eosin–stained sections were photographed with a Zeiss

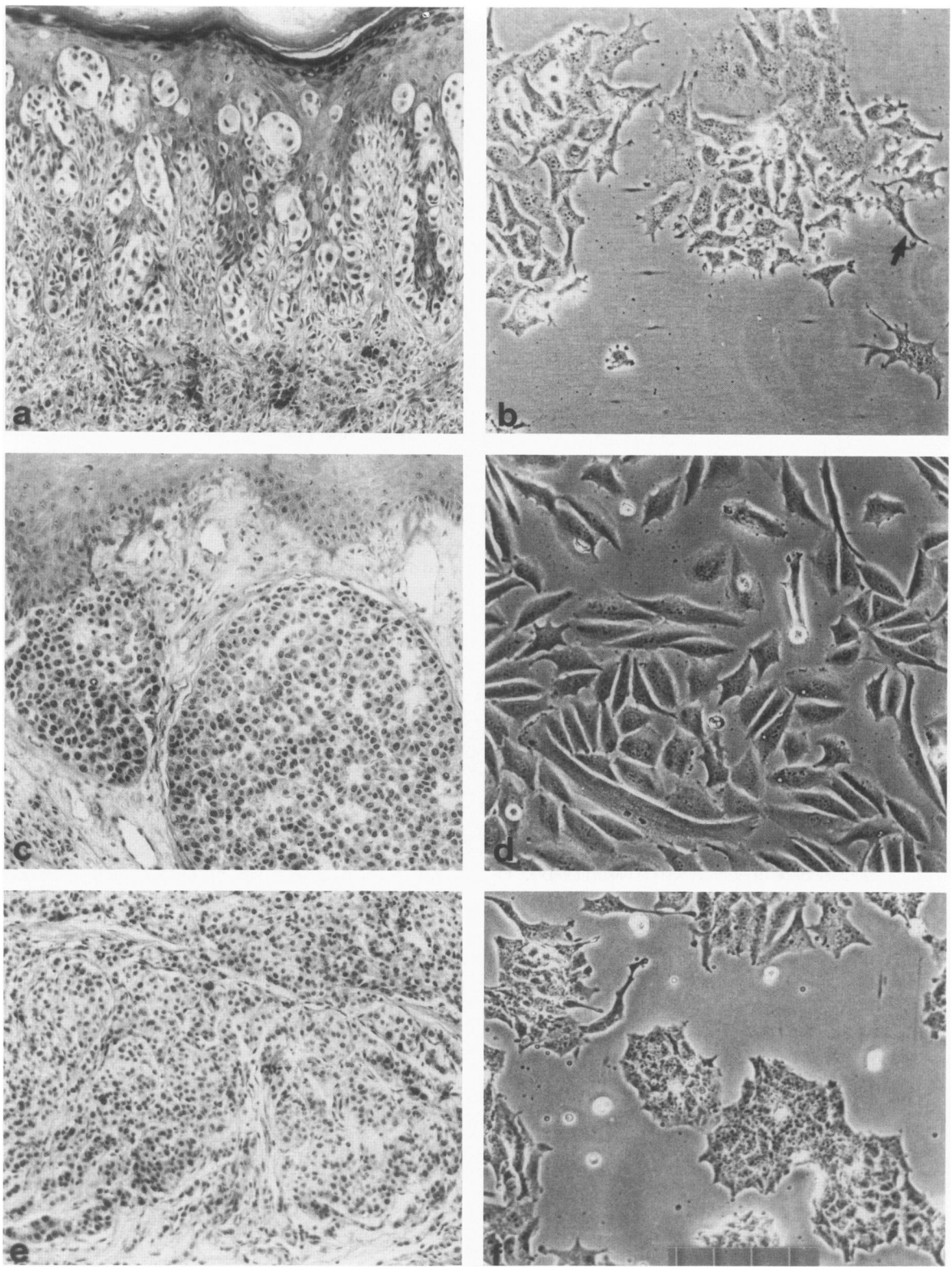

Figure 1. **a**: *Malignant melanoma, superficial spreading type, showing radial growth phase with individual and nested severely atypical nevomelanocytes in a Pagetoid pattern. The section was adjacent to tissue sampled for tissue culture.* **b**: *Primary melanoma cell line PM-WK derived from lesion shown in* **(a)** *at the same magnification (see scale below). Note colony growth pattern of polygonal cells with some cells exhibiting short dendritic processes (arrow).* **c**: *Recurrent primary melanoma revealing large expansile nests of epithelioid cells at the epidermal junction and in the dermis.* **d**: *Recurrent primary melanoma cell line RPM-EP derived from lesion shown in* **(c)**. *Large, well-spread elongated polygonal cells are identified.* **e**: *Recurrent primary melanoma that reveals many cohesive nests in the reticular dermis.* **f**: *Recurrent primary melanoma cell line RPM-MC showing cohesive or colony growth pattern. Scale: 1 division = 50 μm. H&E stain* **(a,c,e)**. *Cultured cells, phase-contrast image* **(b,d,f)**.

compound microscope using the 10× objective and attached 3 × 5 camera back housing using the trinocular port. Cell cultures were photographed with a Nikon FE-2 camera attached to the photo port of the inverted microscope described above using the 10× phase contrast objective.

Fluorescence and Differential Interference Contrast Microscopy

Cells were grown on coverslips, fixed in 4% paraformaldehyde in PBS for 5 minutes, and permeabilized using 0.1% Triton X-100 (Sigma Chemical Co., St. Louis, MO) for 2 minutes. After a rinse in PBS, the cells were incubated for 40 minutes in rhodamine-conjugated phalloidin (Sigma) and rinsed three times in PBS and mounted in a polyvinyl alcohol resin (Lerner Labs, NY). Fluorescent micrography was performed using a Nikon Microphot with an epifluorescent attachment, rhodamine filter cube, a 100-watt UV mercury lamp, and a Plan Apochromat 60× (numerical aperature 1.40) oil objective. The microphot was fitted also with a diascopic differential interference contrast attachment. Photomicrography was performed with an attached automatic camera (Nikon Microflex UFX-II) using 35-mm film (Kodak Tmax 400). The actin-labeled cytoskeleton negative images were projected onto the image analysis digitablet, and the number and length of the stress fibers as well as projected cell surface area were calculated.

Results

The *in situ* cellular morphology of the primary, recurrent primary, and metastatic lesions exhibits cells with the typical malignant phenotype of large nuclei exhibiting nuclear hyperchromasia and pleomorphism. However the amount and shape of the cytoplasm (epithelioid versus spindle), the relation of the cells to one another (cohesive versus dyshesive), and the expression of pigment varies considerably. The most common cell type and pattern observed in the lesions are nonpigmented, cohesive, epithelioid cells with variable amounts of abundant cytoplasm. This histomorphology is seen in primary, recurrent, and metastatic lesions that gave rise to the primary cell line PM-WK, the recurrent cutaneous melanoma cell lines RPM-EP and RPM-MC, and the metastatic cell line MM-LH (Figures 1a, c, e, 3a).Predominantly large pigmented spindle cells are observed in the tissue that gave rise to the cell line MM-AN (Figure 2a) and highly pleomorphic cells in the tissue that grew out MM-BP (Figure 2c). Small dyshesive nonpigmented epithelioid cells are identified in the lymph node that gave rise to the cell line MM-RU (Figure 3c).

Interestingly, the morphology of the cell lines reflect the histomorphology of their *in situ* counterparts. Cell lines PM-WK, RPM-MC, and MM-LH are polygonal cells that grow in cohesive colonies (Figures 1b, f, 3b), whereas RPM-EP is composed of large elongate polygonal cells in colonies with interspersed dyshesive cells (Figure 1d). In contrast, MM-AN is a pigmented spindle cell line, MM-BP is a small pleomorphic cell line with both colonies and dyshesive cells, and MM-RU is composed of dyshesive pleomorphic cells that do not form colonies (Figures 2b, d, 3d).

The primary melanoma cell line (PM-WK) is derived from the epidermis of the radial growth phase. This cell line has been passaged each week for more than 2 years without change in morphology or growth rate. The reticular dermal fragment of the radial growth phase specimen and, surprisingly, tissue of the vertical growth phase did not grow out a stable cell line.

Melanocytes derived from human foreskins are shown in Figure 3e. The cells are predominantly bipolar with occasional tripolar and rare multipolar cells identified. Rare scattered fibroblasts are identified after one treatment with Geneticin. Before migration studies were performed, all fibroblasts were eliminated from subsequent passages by a second Geneticin treatment.

Culture Characterization

All cell lines have exhibited stable morphologies and growth properties for over 70 passages. The doubling times of the cell lines have also been stable and ranged from 1.2 days to 4.8 days. Interestingly at least two groups of proliferation rates can be identified, one rate ranging from a doubling time of 1.2 to 1.5 days and another rate ranging from 2.3 to 4.8 days. Rates of proliferation do not correlate with the stage of progression from whence the tissue is derived. The cell lines with a prominent well-spread or spindle cell component (RPM-EP, MM-AN), however, showed the lower rate of proliferation, whereas the dendritic, polygonal, or pleomorphic cell lines exhibit variable rates of proliferation. No correlation with proliferation rate and migration rate is identified.

All cell lines are confirmed as melanoma cells by either S-100 protein or HMB-45 antigen expression. All cell lines are positive for S-100 protein and all cell lines except MM-RU are positive for HMB-45 after immunoperoxidase labeling. Human fibroblasts are negative for both antigens, whereas normal newborn melanocytes are positive for S-100, yet negative for HMB-45.

Melanoma Cell Spreading and Random Migration

To determine the kinetics of cell spreading and migration after typsinization, random cell migration rates and cell surface areas are calculated at hourly intervals after attachment to the substrate. Attachment was established

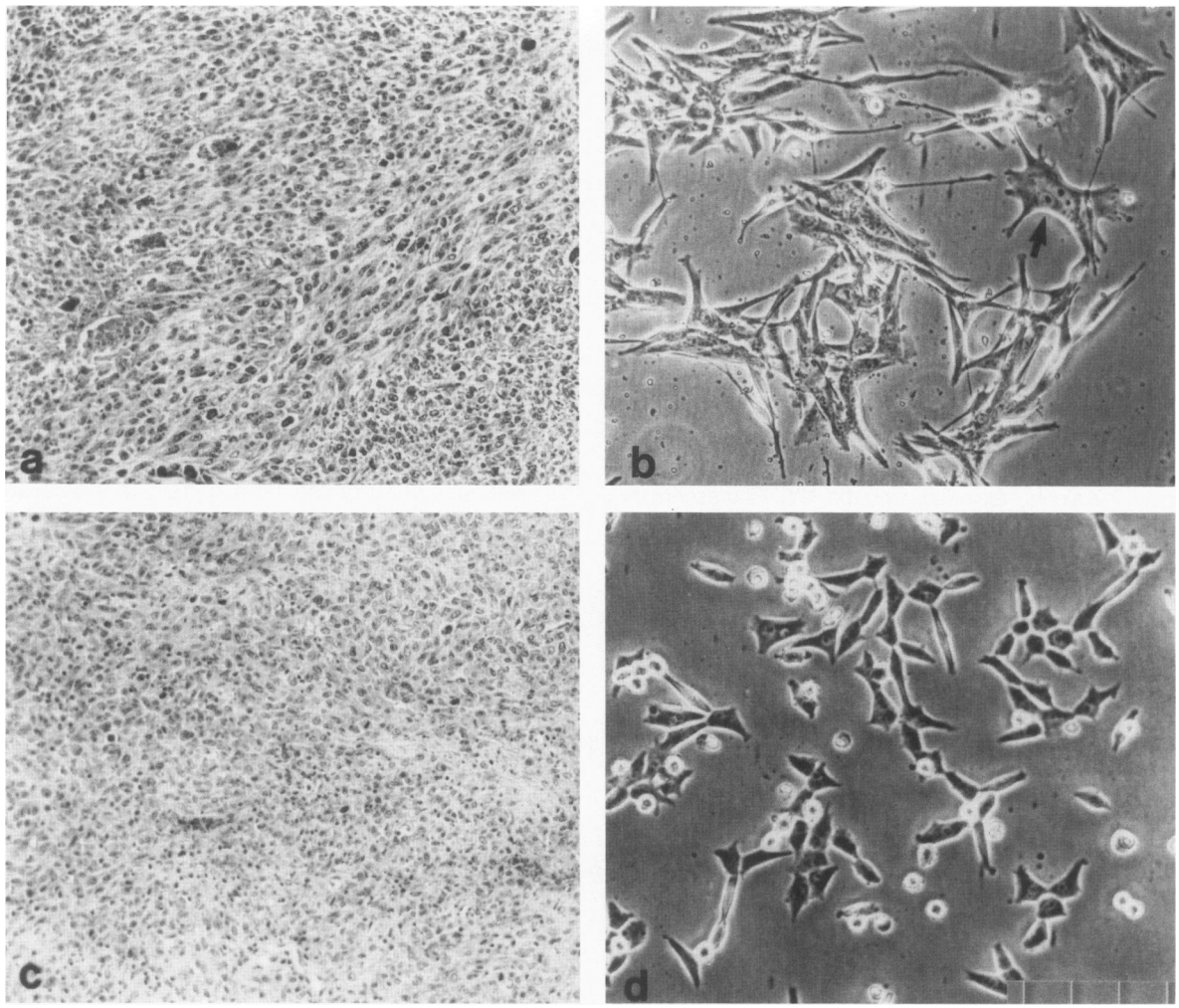

Figure 2. **a**: *Metastatic melanoma to groin lymph node exhibiting spindle cell fascicular pattern with orthogonal arrangement of tumor cells.* **b**: *Metastatic cell line MM-AN derived from* (**a**) *consists of pigmented spindle cells in aggregates with interspersed large multinucleated cells with prominent nucleoli (arrow).* **c**: *Metastatic melanoma to axillary lymph node revealing sheets of small epithelioid cells.* **d**: *Metastatic cell line MM-BP derived from* (**c**) *is composed predominantly of small polygonal cells with interspersed round and some small spindle cells. Scale: 1 division = 50 μm. H&E stain* (**a,c**). *Cultured cells, phase-contrast image* (**b,d**).

after 15 minutes' incubation at 37°C. The results for the cell line MM-RU are shown in Figure 4. Cell spreading is a rapid process in which 85% maximal spreading occurs by 1 hour and 98% by 2 hours (see Figure 4a). Random cell migration exhibits an initial phase of rapid migration followed by a decrease and then stabilization of the migration rate after 2 hours (Figure 4b). All cell lines are recorded after stabilization to permit possible cell surface proteins to regenerate after trypsinization.

Figure 5 illustrates representative tracings obtained from the computer screen of the migration paths of three of the cell lines for a duration of 4 hours. The paths have been normalized to a central starting point as outlined in Methods. These cell lines are chosen only to illustrate the range in the random migration rate observed between the cell lines. The behavior of all cell lines is outlined below.

The mean random translocational migration rates and their respective standard deviations are illustrated in Figure 6 for all melanoma cell lines as well as human newborn foreskin-derived melanocytes. Marked heterogeneity is immediately appreciated among the cell lines. Note the relatively low migration rates of melanocytes, the primary melanoma cell line, one of the recurrent cutaneous cell lines (RPM-MC), and one of the metastatic cell lines (MM-LH). Intermediate migration rates are identified in one of the recurrent primary melanomas (RPM-EP) and two metastatic cell lines (MM-AN and MM-BP). One metastatic cell line (MM-RU) shows a markedly higher rate of migration than all other cell lines. Statistically the rate of migration in the intermediate and highest migrating cell lines are significantly higher than the cell lines with low migration rates ($P < 0.001$; Figure 6 and Table 1).

The distribution of migration rates for all of the cell

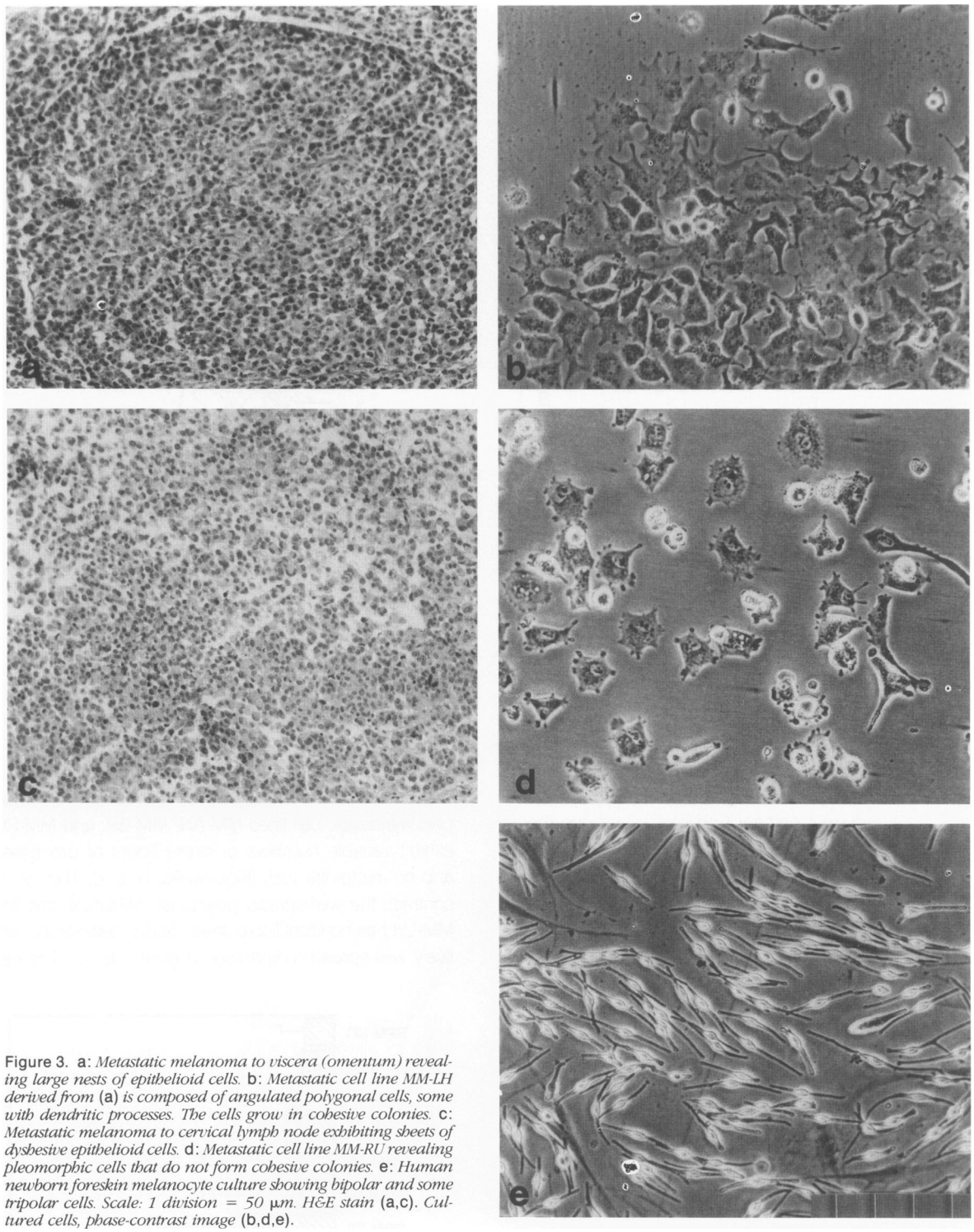

Figure 3. a: *Metastatic melanoma to viscera (omentum) revealing large nests of epithelioid cells.* b: *Metastatic cell line MM-LH derived from* (a) *is composed of angulated polygonal cells, some with dendritic processes. The cells grow in cohesive colonies.* c: *Metastatic melanoma to cervical lymph node exhibiting sheets of dyshesive epithelioid cells.* d: *Metastatic cell line MM-RU revealing pleomorphic cells that do not form cohesive colonies.* e: *Human newborn foreskin melanocyte culture showing bipolar and some tripolar cells. Scale: 1 division = 50 μm. H&E stain* (a,c). *Cultured cells, phase-contrast image* (b,d,e).

lines, expressed as a percentage of total cells within intervals of 10 μm/hour is illustrated in Figure 7. This bar graph demonstrates the diversity of individual cell migration seen among and within cell lines. In addition, the cell lines can be defined into two groups as either low or high random migrators based on the distribution of random cell migration rates: cell lines with less than 10% of their population migrating more than 10 μm/hour are defined as low random migrators, and cell lines with 30% or more of their population migrating more than 10 μm/hour are defined as high random migrators. As seen in the illustration, the melanocytes, primary melanoma cell line (PM-

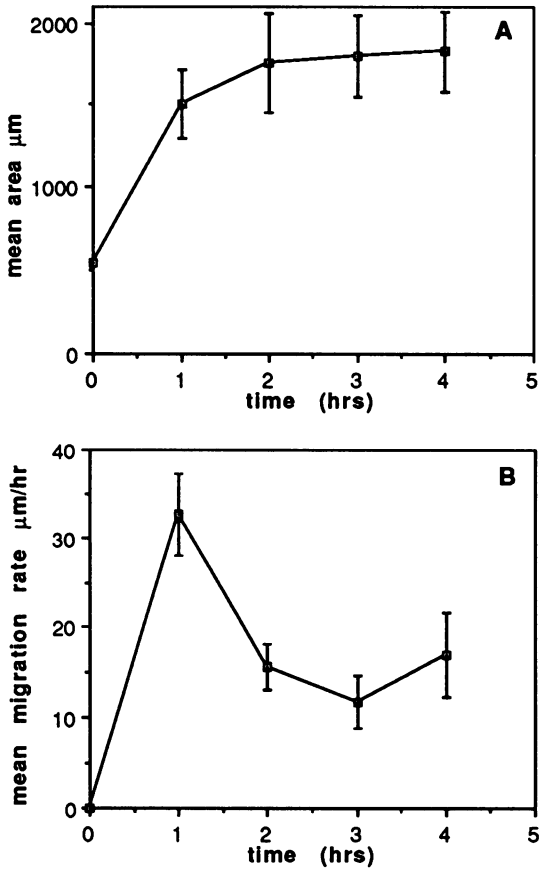

Figure 4. *Relationship of* (a) *cell spreading and* (b) *migration rate as a function of time after trypsinization and plating of the metastatic melanoma cell line MM-RU.*

WK), one recurrent primary (RPM-MC), and one metastatic cell line (MM-LH) are low random migrators. In contrast, three metastatic melanoma cell lines and one recurrent primary melanoma cell line are high random migrators. Only three of these four cell lines exceed 20 μm/hour, however, with maximal observed migration rates of 42, 26, and over 50 μm/hour in the recurrent primary cell line RPM-EP and two metastatic cell lines (MM-AN and MM-RU), respectively.

Actin Distribution and Cell Migration

Reflecting the wide variation in cellular morphology among the cell lines, the distribution of the cytoskeletal protein actin also demonstrates heterogeneity. The presence of actin in stress fiber arrays, as identified by Nomarski differential interference microscopy and fluorescently labeled phalloidin, is not a feature seen in all of the cell lines. In addition, the microvillar arrangement among the cell lines varied considerably.

The primary melanoma cell line (PM-WK, Figure 8a, b) does not form actin bundles in stress fiber arrays, but has many microvilli in tufts (arrow). In contrast, large numbers

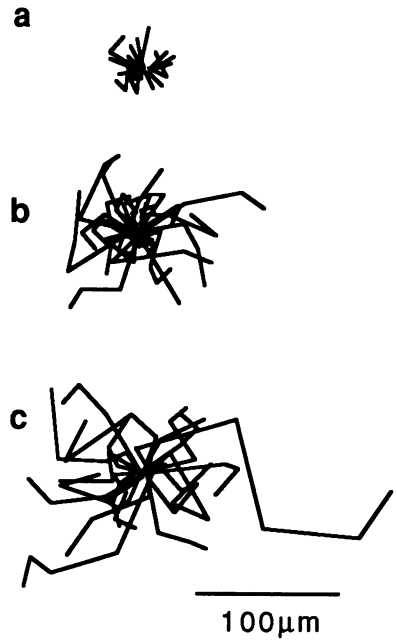

Figure 5. *Normalized random migration paths of three of the cell lines to demonstrate the range of random migration observed.* a: *Primary melanoma cell line PM-WK;* b: *recurrent primary melanoma cell line RPM-EP; and* c: *metastatic cell line MM-RU.*

of actin bundles in stress fiber arrays are seen in the well-spread melanoma cell line derived from one cutaneous recurrence (RPM-EP, Figure 8c, d). Stress fibers are not identified in the other recurrent cutaneous cell line RPM-MC (Figure 8e, f), where instead numerous microvillar tufts are readily identified. The spindle and pleomorphic metastatic cell lines MM-AN, MM-BP, and MM-RU exhibit variable numbers of stress fibers or processes and no microvillar tufts (Figures 9a, b, c, d, 10c, d). In contrast, the well-spread polygonal metastatic cell line MM-LH has no identifiable stress fibers, despite its relatively well-spread morphology (Figure 10a, b). The cell

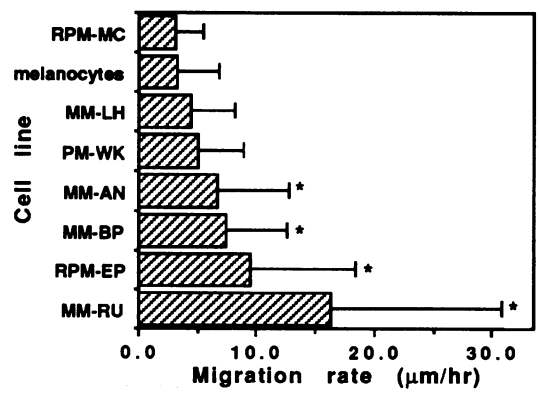

Figure 6. *Mean random migration rate ± SD of the seven human primary, recurrent primary and metastatic cell lines as well as normal human newborn foreskin melanocytes. *Significant difference in migration rate (t-test; P < 0.001) relative to melanocytes, PM-WK, MMLH, or RPM-MC.*

Table 1. *Melanoma Cell Migration,* In Situ *and* In Vitro *Morphology, and Quantitative Morphologic Characteristics of Actin Organization into Stress Fibers*

Melanoma cell line	Mean migration rate (μm/hr)†	% cells migrating >10μm/hr	*In situ* nest formation	*In vitro* colony formation	% Cells with stress fibers	Stress fibers per cell*	Stress fiber length (μm)*	Projected surface area (μm^2)*
RPM-MC	3.1 ± 2.3	2	+	+	0	0	0	643 ± 268
MM-LH	4.4 ± 3.7	5	+	+	0	0	0	1329 ± 614
PM-WK	4.9 ± 3.8	8	+	+	0	0	0	771 ± 391
MM-AN	6.6 ± 6.0†	30	−	−	35	3.1 ± 3.2	11.2 ± 4.6	926 ± 575
MM-BP	7.4 ± 5.1‡	31	−	−	31	5.5 ± 4.1	7.3 ± 3.8	784 ± 361
RPM-EP	9.4 ± 8.9‡	34	−	−	80	28.1 ± 35.9	13.7 ± 7.7	2867 ± 256
MM-RU	16.2 ± 14.6‡	60	−	−	36	5.6 ± 2.8	8.9 ± 4.3	1132 ± 583

* Expressed as ± standard deviation.
† *t*-test; $P < 0.05$ relative to PM-WK, MM-LH and $P < 0.001$ relative to RPM-MC.
‡ *t*-test; $P < 0.001$ relative to PM-WK, MM-LH, and RPM-MC.

surface of MM-LH exhibits many microvilli; however they are not grouped in tufts as found in PM-WK and RPM-MC. Interestingly melanocytes do not demonstrate stress fibers or numerous microvilli; their cytoplasmic processes, however, reveal a diffuse fluorescence, indicating the presence of actin.

Table 1 summarizes the random migration rates, *in situ* and *in vitro* morphology, percentage of cells with actin-containing stress fibers, the average number of stress fibers per cell, the average stress fiber length, and the projected surface area in the seven human malignant melanoma cell lines. A clear relation among the four cell lines that have statistically significantly higher random migration rates, the absence of *in situ* nest formation, the absence of *in vitro* colony formation, and the presence of actin-containing stress fibers is identified. The three metastatic cell lines that had high random migration rates all exhibit a moderate number of cells with stress fibers. The recurrent primary cell line RPM-EP also has a significantly higher rate of migration and demonstrates the highest number of cells with stress fibers as well as number of stress fibers per cell. This cell line also has the largest projected substrate surface area of all seven cell lines. Conversely no relation between stress fibers and projected surface area in the other cell lines is identified. In fact, well-spread cells may not form stress fibers, as evident in the cell line MM-LH, which has the second largest projected surface area. This cell line, however, has few cells migrating more than 10 μm/hour.

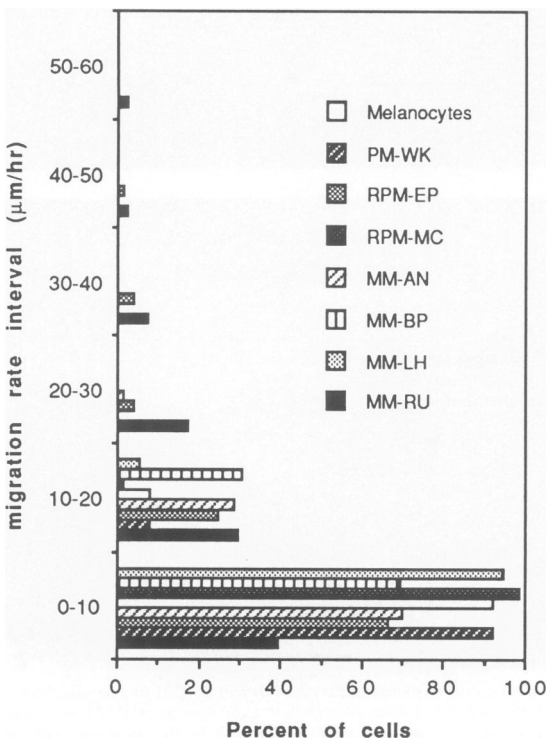

Figure 7. *Distribution of random migration rates of newborn foreskin melanocytes and the seven human primary, recurrent primary, and metastatic cell lines, demonstrating heterogeneity of migration rates among and within cell lines.*

Discussion

Early studies on the distribution of actin filaments in transformed or malignant cultured cells found that a decrease in microfilament bundles (stress fibers) correlated with tumorigenicity; however numerous exceptions were identified in certain cell lines (for review of the older literature see reference 14). More recently, however, fewer stress fibers were reported in certain murine and human melanoma cell lines that showed a greater malignant potential than those with a lower metastatic potential as defined by lung colonization numbers after tail vein injection in syngeneic or immunodeficient mice.[7,8] The B16-F1 mouse melanoma cell line exhibits more actin cables (stress fibers) and elicits fewer metastases than the B16-F10 cell line.[6] The mechanisms underlying these differences are unclear, but likely involve a combination of actin-associated proteins, regulatory elements, or actin itself. Indeed certain isoforms of actin in the mouse model recently have been identified that are downregulated in the

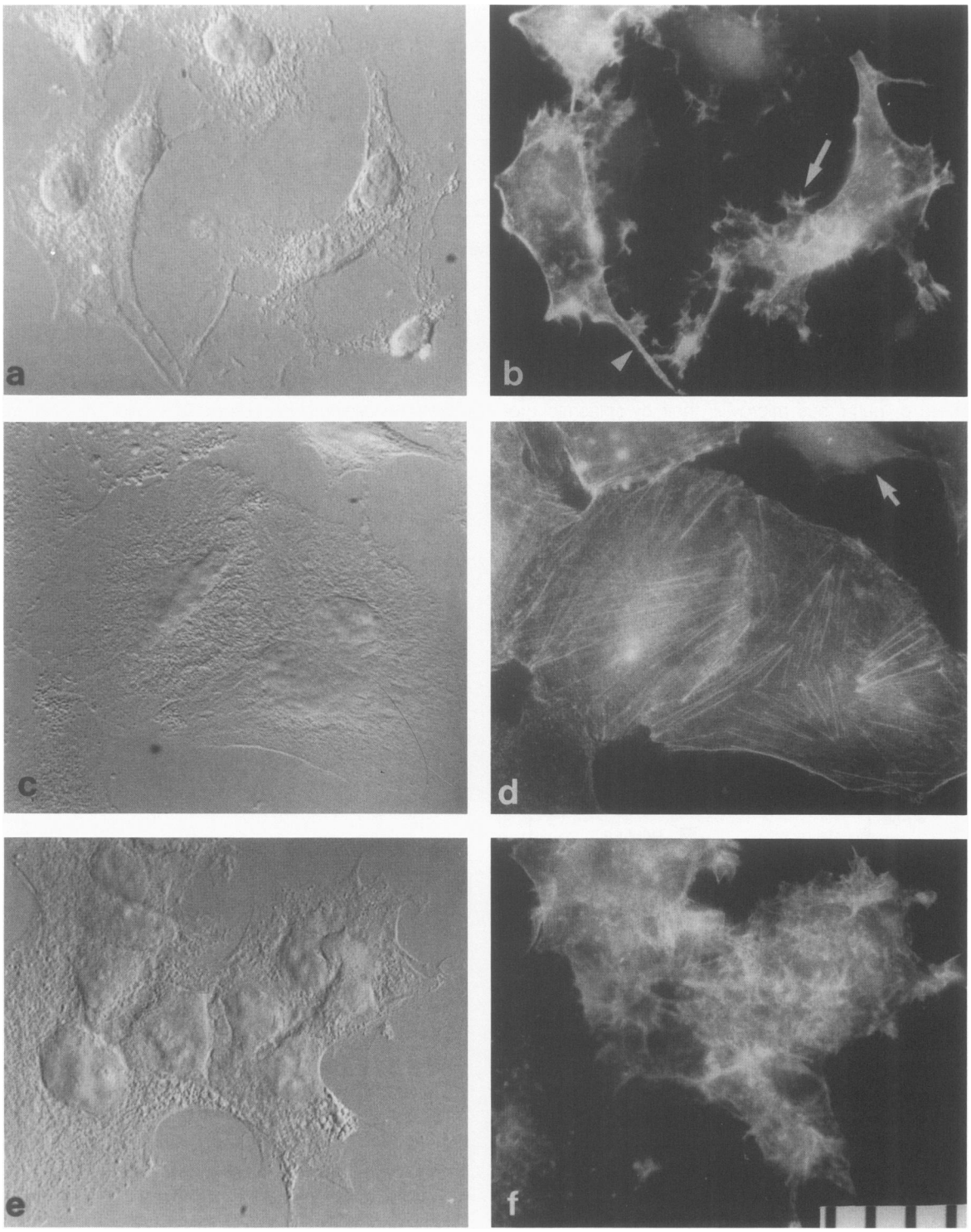

Figure 8. *Normarski differential interference contrast image* **(a,c,e)** *and fluorescently labeled actin distribution* **(b,d,f)** *in human primary and recurrent melanoma cell lines. The primary melanoma cell line PM-WK exhibits many microvillar tufts (arrows) and some actin-containing dendritic processes (arrowhead). No stress fiber is identified. The large number of well-spread cells in the recurrent cell line RPM-EP* **(c,d)** *show actin organized into stress fibers, whereas some less well-spread cells do not (arrow). The cell line RPM-MC* **(e,f)** *shows colonies with cells with actin organized into microvillar tufts and microspikes. Scale: 1 division = 10 μm.*

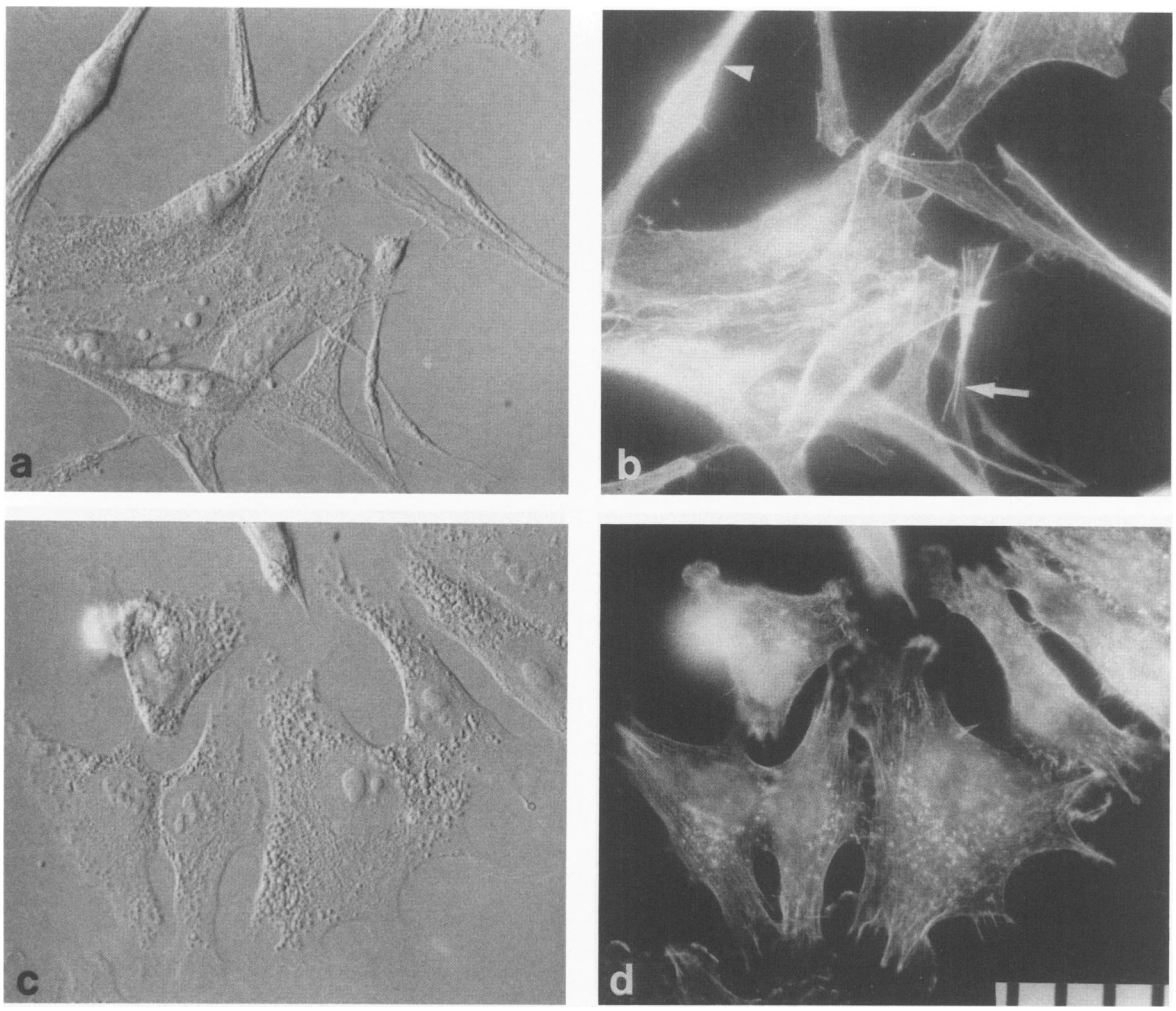

Figure 9. *Normarski differential interference contrast image* (a,c,) *and fluorescently labeled actin distribution* (b,d) *in human metastatic melanoma cell lines. The pigmented spindle cell line MM-AN* (a) *contains both spindle and well-spread cells with and without stress fibers (arrows, arrowheads, respectively). The metastatic cell line MM-BP has many cells with short stress fibers and other cells that do not* (d). *Scale: 1 division = 10 μm.*

lines with greater metastatic potential,[15] and other isoforms of actin have been identified that are present in human benign nevi but not in human malignant melanoma.[16] These isoforms may play a role in the organization of actin in melanoma cells and alter cell migration.

To investigate the relation of the organization of actin and metastases in human malignant melanoma, we isolated seven human melanoma cell lines from different stages of tumor progression. Our hypothesis, based on the experimental model systems to date, was that metastatic cell lines would have fewer stress fibers than those isolated from earlier stages of progression. This hypothesis was not confirmed; indeed stress fibers were a more frequent finding in metastatic melanoma. Nevertheless our findings do not necessarily contradict the mouse model studies because those injected melanoma cells, whether of low or high malignant potential, may be considered to be metastatic nonetheless, and do in fact exhibit stress fibers. Our surprising finding is the absence of stress fibers in some of our human melanoma cell lines.

The human primary melanoma cell line PM-WK, derived from the radial growth phase, did not exhibit stress fibers even though it was derived from a lesion with a relatively low malignant potential.[3] Of the two recurrent cutaneous melanoma cell lines, one exhibited numerous actin bundles in stress fiber arrays and the other did not. Finally three of four metastatic melanoma cell lines exhibited stress fiber formation in a significant number of cells. These findings may suggest that stress fibers are identified in cells derived from later stages of tumor progression. Indeed human newborn foreskin melanocytes did not demonstrate stress fibers and showed significantly lower migration rates.

The striking relationship of a melanoma cell line's expression of actin bundles in the form of stress fibers and

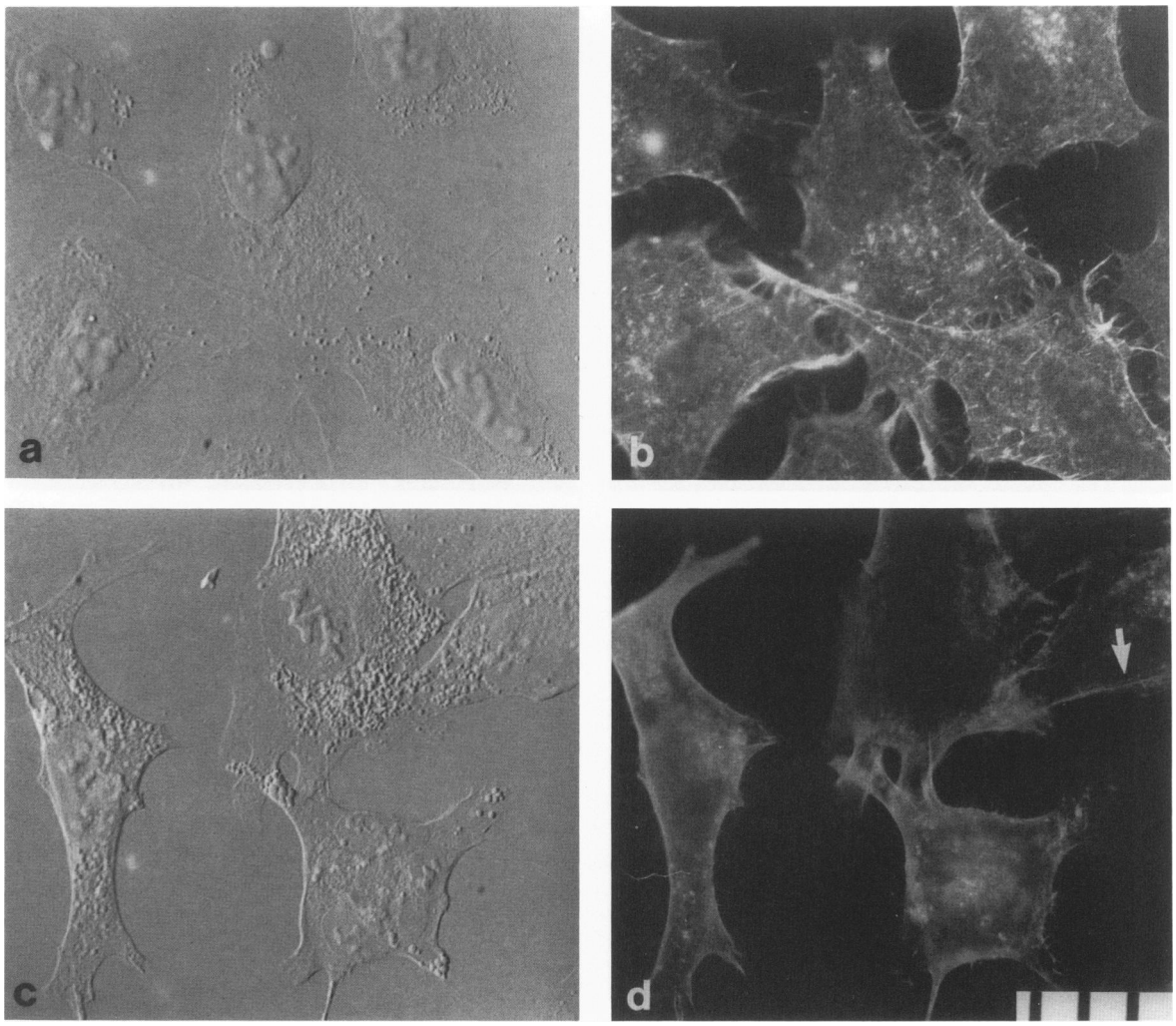

Figure 10. *Normarski differential interference contrast image* (**a,c**) *and fluorescently labeled actin distribution* (**b,d**) *in human metastatic melanoma cell lines. The metastatic cell line MM-LH consists of many well-spread cells* (**a**) *that do not have actin organized into stress fibers* (**b**). *Microvilli and microspikes are prominent. The pleomorphic metastatic cell line MM-RU* (**c**) *shows rare microvilli and occasional short actin-containing fibers* (**d**, *arrows*). *Scale: 1 division = 10 μm.*

significantly higher random migration rates is demonstrated in this study. In addition, the presence of numerous microvilli or tufts of microvilli correlated with low random migration rates. The remarkable morphologic similarities between the cells *in situ* and *in vitro* may reflect both the organization of their cytoskeletons and the ability of the cells to migrate. The formation of nests *in situ* was correlated with colony formation *in vitro*, and colony formation results in part, from low random migration rates. If cells have a high random migration rate, the cells separate from each other after cell division and hence colony formation is not observed.

The isolation of human primary, recurrent cutaneous, and metastatic melanoma cell lines that are characterized in relation to cell spreading, actin organization, and cell migration may provide a valuable model to investigate further aspects of tumor progression. Recent investigators have successfully used cell culture in the analysis of precursors of primary melanoma and the tumorigenic phase of primary melanoma to test metastatic potential in immunodeficient mice.[17] The heterogeneity expressed by these cell lines with regard to random cell migratory behavior and actin organization may provide insight into the expression of cell adhesion molecules, factors influencing metastasis in the immunodeficient mouse, and the interpretation of invasion assay systems using extracellular matrix-coated micropore filters[4] or human amnionic membrane.[18]

The marked heterogeneity of melanoma cell migration and actin organization seen among cell lines in this study speaks for caution in the interpretation of data from one or two cell lines. Likewise the wide distribution of migration rates and variation of actin organization within each cell line speaks for individual cell heterogeneity. Nevertheless

a consistent finding is that stress fibers are identified only in the cell lines with significantly higher mean random migration rates. This is unexpected in view of studies correlating decreased motility with high numbers of stress fibers and focal contacts. Heterogeneity within a cell line may explain the apparent paradox. Indeed, although rapidly migrating fibroblasts have been shown to exhibit few stress fibers and slowly migrating well-spread cells have numerous stress fibers, fibroblasts nevertheless have high mean random migration rates.[19,20] The formation of actin bundles in stress fiber arrays in some of the cells does not preclude others from exhibiting rapid cell migration. The fact that high migration rates are detected in fibroblasts, keratinocytes,[21] and endothelial cells[22] likely reflects their important migratory role in reparative processes.

Benign human newborn melanocytes and the primary melanoma cell line have low migration rates relative to most of the melanoma cell lines isolated from later stages of tumor progression. It is possible that melanoma cells with the highest migration rates are the first to reach the lymphatics. Further selection, cloning, and characterization of elements such as adhesion molecules and cytoskeletal protein expression may provide insight into the role of cell migration in metastasis.

Acknowledgments

The authors thank members of the Department of Surgery, including Drs. A. Benedict Cosimi, Ronald Malt, William Wood, and William Gallagher and members of the Department of Dermatology, including Drs. Jessica Fewkes and Stuart Salasche, for their supply of fresh tissue for this study.

References

1. Clark WH, Elder DE, Guerry D, Epstein MN, Greene MH, VanHorn M: A study of tumor progression. The precursor lesions of superficial spreading and nodular melanoma. Hum Pathol 1984, 15:1147–1165
2. Clark WH, Elder DE, VanHorn M: The biologic forms of malignant melanoma. Hum Pathol 1986, 17:443–450
3. Clark WH, Elder DE, Guerry D, Braitman LE, Trock BJ, Schultz D, Synnestvedt M, Halpern AC: Model predicting survival in stage I melanoma based on tumor progression. J Natl Cancer Inst 1989, 81:1893–1904
4. Liotta LA, Wewer U, Rao NC, Schiffman E, Stracke M, Guirguis R, Thorgeirsson U, Muschel R, Sobel M: Biochemical mechanisms of tumor invasion and metastases. Adv Exp Med Biol 1988, 233:161–169
5. Nabi IR, Raz A: Loss of metastatic responsiveness to cell shape modulation in a newly characterized B16 melanoma adhesive cell variant. Cancer Res 1988, 48:1258–1264
6. Raz A, Geiger B: Altered organization of cell-substrate contacts and membrane-associated cytoskeleton in tumor cell variants exhibiting different metastatic capabilities. Cancer Res 1982, 42:5183–5190
7. Raz A: Actin organization, cell motility, and metastasis. Adv Exp Med Biol 1988, 233:227–233
8. Volk T, Geiger B, Raz A: Motility and adhesive properties of high- and low-metastatic murine neoplastic cells. Cancer Res 1984, 44:811–824
9. Zachary JM, Cleveland G, Kwock L, Lawrence T, Weissman RM, Nabell L, Fried FA, Staab EV, Risinger MA, Lin S: Actin filament organization of the Dunning R3327 rat prostatic adenocarcinoma system: Correlation with metastatic potential. Cancer Res 1986, 46:926–932
10. Raz A, Zoller M, Ben Z: Cell configuration and adhesive properties of metastasizing and non-metastasizing BSp73 rat adenocarcinoma cells. Exp Cell Res 1986, 162:127–141
11. Young MR, Newby M, Meunier J: Relationships between morphology, dissemination, migration, and prostaglandin E2 secretion by cloned variants of Lewis lung carcinoma. Cancer Res 1985, 45:3418–3423
12. Badenoch-Jones P, Ramshaw IA: Spontaneous capillary tube migration of metastatic rat mammary adenocarcinoma cells. Invasion Metastasis 1984, 4:98–110
13. Halaban R, Alfano FD: Selective elimination of fibroblasts from cultures of normal human melanocytes. In Vitro 1984, 20:447–450
14. Byers HR, White GE, Fujiwara K. Organization and function of stress fibers in cells *in vitro* and *in situ:* A review, Cell and Muscle Motility. Edited by R Dowben, J Shay. New York, Plenum Press, 1984, pp 83–137.
15. Taniguchi S, Sadano H, Kakunaga T, Baba T: Altered expression of a third actin accompanying lignant progression in mouse B16 melanoma cells. Jpn J Cancer Res 1989, 80:31–40
16. Sasase A, Mishima Y, Ichihashi M, Taniguchi S: Biochemical analysis of metastasis-related Ax actin in B16 mouse melanoma cells after chemical reversional modulation and of tumor progression-related A′ actin in the ontogeny of human malignant melanoma. Pigment Cell Res 1989, 2:493–501
17. Herlyn M, Thurin J, Balaban G, Bennicelli JL, Herlyn D, Elder DE, Bondi E, Guerry D, Nowell P, Clark WH, Koprowski H: Characteristics of cultured human melanocytes isolated from different stages of tumor progression. Cancer Res 1985, 45:5670–5676
18. Hendrix MJ, Seftor EA, Seftor RE, Misiorowski RL, Saba PZ, Sundareshan P, Welch DR: Comparison of tumor cell invasion assays: Human amnion versus reconstituted basement membrane barriers. Invasion Metastasis 1989, 9:278–297
19. Lewis L, Verna J-M, Levinstone D, Sher S, Marek L, Bell E: The relationship of fibroblast translocations to cell morphology and stress fibre density. J Cell Sci 1982, 53:21–36
20. Herman IM, Crisona NJ, Pollard TD: Relation between cell activity and distribution of cytoplasmic actin and myosin. J Cell Biol 1981, 90:84–91
21. Nickoloff BJ, Mitra RS, Dixit VM, Varani J: Modulation of keratinocyte motility. Am J Pathol 1988, 132:543–551
22. Sharpe RJ, Byers HR, Scott FS, Bauer SI, Maione TE: Growth inhibition of murine melanoma and human colon carcinoma by recombinant human platelet factor 4 in the mouse. J Natl Cancer Inst 1990, 82:848–53